Handbook of Modern Biophysics

Thomas Jue
Kazumi Masuda
Editors

Application of Near Infrared Spectroscopy in Biomedicine

Springer

Handbook of Modern Biophysics

Thomas Jue
Kazumi Masuda
Editors

Application of Near Infrared Spectroscopy in Biomedicine

Springer

Handbook of Modern Biophysics

Series Editor
Thomas Jue
University of California Davis
Davis, California

For further volumes:
http://www.springer.com/series/7845

Thomas Jue • Kazumi Masuda
Editors

Application of Near Infrared Spectroscopy in Biomedicine

Volume 4

Springer

Editors
Thomas Jue
Biochemistry and Molecular Medicine
University of California Davis
Davis, CA, USA

Kazumi Masuda
Kanazawa University
Kanazawa, Japan

ISBN 978-1-4614-6251-4 ISBN 978-1-4614-6252-1 (eBook)
DOI 10.1007/978-1-4614-6252-1
Springer New York Heidelberg Dordrecht London

Library of Congress Control Number: 2012956439

Printed on acid-free paper

Springer is part of Springer Science+Business Media (www.springer.com)

Preface

The advent of near-infrared spectroscopy (NIRS) presents a unique tool for understanding the regulation of oxidative metabolism during the transition from rest to an active state. Many laboratories have started to apply NIRS to interrogate both cerebral and muscle metabolism and have garnered insights to discriminate the bioenergetics and hemodynamics of healthy and diseased tissue. Yet using NIRS technology and methodology appropriately requires a solid understanding of the principles of physics, biochemistry, and physiology. Indeed, introducing a complex biophysics topic in an academically rigorous but interesting way often poses a challenge.

In keeping with the style of the *Handbook of Modern Biophysics*, the current volume balances the need for physical science/mathematics formalism with a demand for biomedical perspectives. Each chapter divides the presentation into two major parts: the first establishes the conceptual framework and describes the instrumentation or technique, while the second illustrates current applications in addressing complex biology questions. With the additional sections on further reading, problems, and references, the interested reader can explore some chapter ideas more widely.

In the fourth volume in this series, *Application of Near-Infrared Spectroscopy in Biomedicine*, the authors have laid down a solid biophysical foundation. Masatsugu Niwayama and Yutaka Yamashita open by delineating the different types of NIRS methods, describing different instrumentations, and explaining the underlying idea about photon migration. Eiji Okada expands on the key concept of photon migration, especially as it applies to brain imaging. Hajime Miura surveys the application of NIRS in the clinic, while Takafumi Hamaoka describes the use of NIRS in studying human locomotion. Kazumi Masuda explores the use of NIRS to understand regulation of intracellular and vascular oxygen from the start of muscle contraction. Williams and Ponganis show the unique application of NIRS to investigate oxygen regulation in marine mammals during a breathhold or a dive. Finally, Chung and Jue compare the use of NIRS and NMR in determining the role of intracellular oxygen during muscle contraction.

This volume continues the philosophy behind the *Handbook of Modern Biophysics* in providing the reader with a fundamental grasp of concepts and applications on current biophysics topics.

Davis, CA, USA — Thomas Jue

Contents

Contributors

Youngran Chung Biochemistry and Molecular Medicine, University of California Davis, Davis, CA 95616-8635, USA

Miura Hajime Laboratory for Applied Physiology, University of Tokushima, Tokushima 770-8502, Japan

Takafumi Hamaoka Department of Sport and Health Science, Ritsumeikan University, 1 Nojihigashi, Kusatsu, Shiga, Japan

Thomas Jue Biochemistry and Molecular Medicine, University of California Davis, Davis, CA 95616-8635, USA

Kazumi Masuda Faculty of Human Sciences, Kanazawa University, Kanazawa, Ishikawa 920-1192, Japan

Masatsugu Niwayama Department of Electrical and Electronic Engineering, Shizuoka University, 3-5-1 Johoku, Nakaku, Hamamatsu, Shizuoka 432-8561, Japan

Eiji Okada Department of Electronics and Electrical Engineering, Keio University, Yokohama 223-8522, Japan

Paul J. Ponganis Center for Marine Biomedicine and Biotechnology, Scripps Institution of Oceanography, University of California San Diego, La Jolla, CA 92093-0204, USA

Cassondra L. Williams Department of Ecology and Evolutionary Biology, University of California Irvine, 321 Steinhaus, Irvine, CA 92697-2525, USA

Yutaka Yamashita Central Research Laboratory, Hamamatsu Photonics KK, 5000 Hirakuchi, Hamakita-ku, Hamamatsu City, Shizuoka 434-8601, Japan

Principles and Instrumentation

1

Yutaka Yamashita and Masatsugu Niwayama

1.1 Light Absorption and Light Scattering

Quantification of chromophore concentration is based on the Beer-Lambert law [1–3]. In Fig. 1.1 the absorption coefficient μ_a is defined as

$$dI = -\mu_a \, I \, dl, \tag{1.1}$$

where dI is the change in intensity I of light moving along an infinitesimal path dl in a homogeneous medium. Integration over a thickness l (mm) yields

$$I_1 = I_0 \exp(-\mu_a \, l), \tag{1.2}$$

where I_0 is the incident light intensity. This equation is also expressed as base 10 logarithms as

$$I_l = I_0 \; 10^{-c\varepsilon l}. \tag{1.3}$$

Where c is the concentration of the compound, and ε is the molar absorption coefficient.

Transmission T is defined as the ratio of the transmitted light intensity to the incident light intensity, I_1/I_0. The optical density (OD) is given by

$$\mathrm{OD} = \log 10(1/T) = \log 10(I_0/I_1). \tag{1.4}$$

Y. Yamashita, BS
Central Research Laboratory, Hamamatsu Photonics KK, 5000 Hirakuchi,
Hamakita-ku, Hamamatsu City,
Shizuoka 434-8601, Japan
e-mail: yutaka@crl.hpk.co.jp

M. Niwayama, Ph.D. (✉)
Department of Electrical and Electronic Engineering, Shizuoka University,
3-5-1 Johoku, Nakaku, Hamamatsu, Shizuoka 432-8561, Japan
e-mail: tmniway@ipc.shizuoka.ac.jp

T. Jue and K. Masuda (eds.), *Application of Near Infrared Spectroscopy in Biomedicine*,
Handbook of Modern Biophysics 4, DOI 10.1007/978-1-4614-6252-1_1,

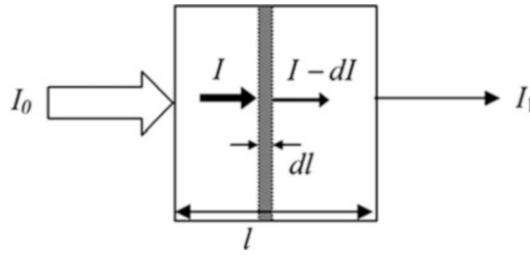

Fig. 1.1 Light transmission through a nonscattering medium

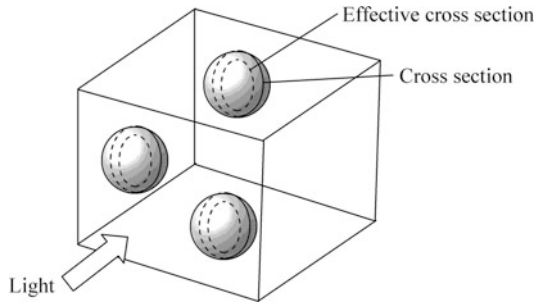

Fig. 1.2 Effective cross-section related to the scattering coefficient

When OD and ε are expressed as base 10 logarithms, the following expression is obtained from Eqs. 1.2, 1.3, and 1.4:

$$\mathrm{OD} = c\varepsilon l = \log_{10}(\mathrm{e})\ \mu_a l, \tag{1.5}$$

where $\log_{10}(\mathrm{e})$ is 0.43429.

Scattering of light in biological tissue is caused by refractive index mismatches at boundaries, such as cell membranes and organelles. The area that contributes to scattering is called the effective cross-section, as depicted in Fig. 1.2. The scattering coefficient μ_s (mm^{-1}) is expressed as the cross-sectional area (mm^2) per unit volume of the medium (mm^3). When the scattered photon does not return to the incident axis, μ_s can be defined as

$$I = I_0 \exp(-\mu_s l). \tag{1.6}$$

The scattering path length, defined as $1/\mu_s$, is the expected value of distance that a photon travels between scattering events and defines the distance that reduces incident light I_0 to I_0/e due to scattering. The total attenuation coefficient, μ_t is defined as the sum of the absorption and scattering coefficients, and $1/\mu_t$ is called the mean free path. When a photon is incident along the direction **i**, the angular probability of the photon being scattered in the direction **s** is given by the phase function f(**i**,**s**). The phase function is conventionally expressed as a function of the cosine of the scattering angle. The anisotropy can be represented as the mean cosine of the scattering angle, and the anisotropy factor g is defined as

$$g = \int_{-1}^{1} \cos\theta\, f(\cos\theta) d\cos\theta. \tag{1.7}$$

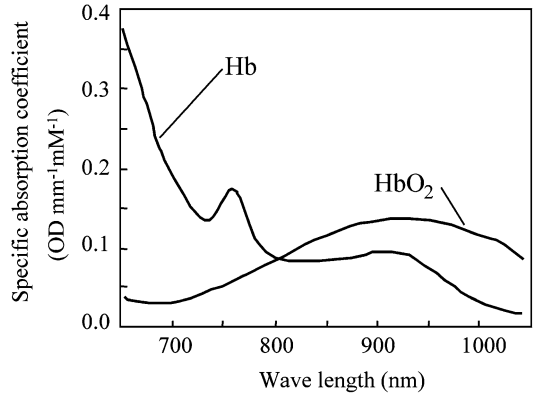

Fig. 1.3 Absorption spectra of oxyhemoglobin and deoxyhemoglobin

When $g = 0$ scattering is isotropic. Moreover, when $g = 1$ the incident light travels in a straight line. In contrast, when $g = -1$ complete backward scattering is observed. Biological tissues arestrongly forward-scattering media ($0.69 < g < 0.99$). The reduced scattering coefficient (μ'_s) is defined using the anisotropy factor as follows:

$$\mu'_s = \mu_s(1 - g). \tag{1.8}$$

The reduced scattering coefficient can be interpreted as representing the equivalent isotropic scattering coefficient and is used for the diffusion theory or Monte Carlo simulation when assuming isotropic scattering.

1.2 Optical Properties of Tissue

Hemoglobin is an iron-containing protein in red blood cells. One mole of deoxygenated hemoglobin (Hb) binds with four moles of oxygen to become oxygenated hemoglobin (HbO_2). The absorption spectra of oxygenated hemoglobin and deoxygenated hemoglobin [4] are shown in Fig. 1.3. The curves of the two hemoglobins intersect at about 800 nm, and the crossing point is called the isosbestic point. Since myoglobin and hemoglobin have similar absorption spectra, it is not easy to distinguish concentrations with spectroscopy. The separation of absorbers is also described in §1.4.

The absorption coefficient for water [5] is shown in Fig. 1.4. The absorption of water is small at wavelengths between about 200 and about 900 nm. Considering all components related to absorption in biological tissues, measurements at wavelengths between 680 and 950 nm are particularly suitable for spectroscopy.

Although many values for the optical properties of muscle and the overlying tissues (fat and skin) have been reported, there are significant differences in the results depending on the method of tissue preparation (fresh, saline-immersed, frozen, or thawed) and the theoretical analysis (diffusion theory, adding–doubling, Monte Carlo lookup tables). In Table 1.1 the optical properties of muscle, fat, dermis, and epidermis at wavelengths between 630 and 850 nm are given.

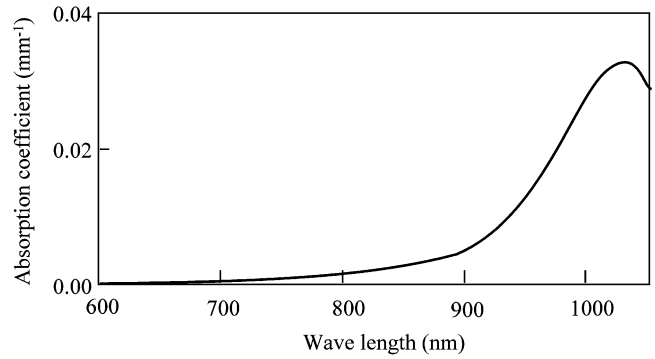

Fig. 1.4 Absorption spectrum of water

Table 1.1 Optical properties of muscle, fat, bone, dermis, and epidermis

Sample	λ (nm)	μ_a (mm^{-1})	μ_s' (mm^{-1})	References
Muscle				
Human forearm (in vivo)	800	0.015	1.0	Ferrari [6]
Human forearm (in vivo)	825	0.021–0.027	0.45–0.87	Zaccanti [7]
Human calf (in vivo)	825	0.018–0.028	0.51–0.85	Zaccanti [7]
Bovine muscle (in vitro)	633	0.096	0.53	Kienle [8]
Bovine muscle (in vitro)	751	0.037	0.34	Kienle [8]
Human calf (in vivo)	800	0.017 ± 0.005	0.80–1.1	Matcher [9]
Fat				
Human mamma (in vivo)	800	0.0017–0.0032	0.72–1.22	Mitic [10]
Human mamma (in vivo)	800	0.0023–0.0026	0.80–1.1	Suzuki [11]
Bovine fat (in vitro)	751	0.0021	1.0	Kienle [8]
Bone				
Pig skull (in vitro)	650	0.05	2.6	Firbank [12]
Pig skull (in vitro)	960	0.04	1.32	Firbank [12]
Human skull (in vivo)	849	0.022	0.91	Bevilacqua [13]
Dermis				
Pig dermis (in vitro)	790	0.018	1.4	Beek [14]
Pig dermis (in vitro)	850	0.033	0.9	Beek [14]
Epidermis				
Pig epidermis (in vitro)	790	0.24	1.9	Beek [14]
Pig epidermis (in vitro)	850	0.16	1.4	Beek [14]

1.3 Near-Infrared Spectroscopy

Spectroscopic measurement of in vivo tissue was first studied by Nicolai et al. [15] in 1932. They examined the optical characteristics of hemoglobin. The first practical ear oximeter for aviation use was developed by Millikan [16] ten years later. In 1949 Wood and Geraci [17] modified this instrument to obtain absolute values of oxygen saturation of arterial blood. The basic idea of this instrument was used to manufacture ear oximeters that were used in clinical settings until the 1970s. However, they did not have sufficient measurement stability for continuous monitoring of oxygen saturation because the calibration procedures were based on various extraneous assumptions. In 1974 Aoyagi et al. [18] presented a new idea called pulse oximetry, which utilizes the pulsation of arteries. This allowed for accurate measurement of oxygen saturation of arterial blood without the influence of